A nonlinear global model of single frequency capacitively coupled plasma and its experimental validation

P. Saikia,[1,a] H. Bhuyan,[1] M. Escalona,[1] M. Favre,[1] R. S. Rawat,[2] and E. Wyndham[1]

[1]*Institute of Physics, Pontificia Universidad Católica de Chile, Av. Vicuña Mackenna 4860, Santiago, Chile*

[2]*National Institute of Education, Nanyang Technological University, Singapore*

(Received 17 January 2018; accepted 29 March 2018; published online 13 April 2018)

The behavior of a single frequency capacitively coupled plasma (CCP) driven by 13.56 MHz rf source is investigated using an approach that integrates a nonlinear global analytical model and experimental data. The non linear model consists of a description of the plasma bulk, based on a fluid dynamics approach coupled to a separate model of the sheath. The parameters used in the model are obtained by operating the single frequency CCP experiment (13.56 MHz) in argon at working pressures 73 to 400m torr. Experimentally measured plasma parameters such as the electron density, electron temperature, the discharge symmetry parameter as well as the rf voltage waveforms are the inputs of the theoretical model. Model results of the DC self bias and rf current for various operating pressures and powers are shown. A comparison of the outputs of the numerical results is done with the experimentally obtained values of the DC self bias and rf current. A good quantitative correspondence between them is obtained. The results presents may substantially improve the understanding of the behavior of the capacitively coupled plasma. https://doi.org/10.1063/1.5022654

I. INTRODUCTION

In the last few decades, radio frequency (rf) discharge has found importance in the fundamental as well as in the experimental research.[1–4] There have been many studies using different configurations, among these most frequently used are capacitively coupled plasma (CCP) and inductively coupled plasma (ICP). Due to the energetic ions, chemically active species, radicals and also energetic neutral species, CCP is extensively used as a low temperature plasma processing medium for material processing in many fields.[5–7] The CCP discharges are widely studied for various applications in different pressure regimes, ranging from few mTorrs to atmospheric pressure.[8,9] Most of the CCPs used in processing applications carried out by a single frequency source at 13.56 MHz. However, recently in some of the CCP research of practical interest in the etching industry, a low frequency source of 1 or 2.26 MHz is also used.[10]

Due to the presence of the non linearity, the characteristics of the CCP sheath are much more complex than the DC sheath.[11–13] An analytical model is therefore, indispensable to understand the dynamics of the rf sheath. Here, we have used an analytical model, where the description of the plasma bulk based on a fluid dynamics approach is coupled to a separate sheath model that takes its nonlinear charge voltage characteristics into account. Mussenbrock et al. first applied such a model to explain the self excitation of the plasma series resonance by the nonlinearities of the boundary sheath.[14] In our previous publication, we have modified the model by considering the sheath at the grounded electrode taking account the finite geometrical asymmetry of the chamber.[15–18]

[a]Electronic mail: partha.008@gmail.com

Well developed Particle in cell/Monte Carlo codes (PIC/MCCs) are now available to study CCPs under a wide range of operating parameters.[19,20] But we have preferred the voltage driven analytical approach over the PIC/MCCs to study such type of discharges. Faster convergence rate of the analytical models compared to the PIC/MCCs is one of the reasons that motivate us to use such an approach. In addition to the faster convergence, an analytical model allows to determine the dominant physics, whereas a PIC/MCC simulation initially does not allow doing this without further analysis. Although several numerical and simulation studies have been done in the recent years, which are based on the Mussenbrocks seminal work,[15–18] few experimental reports are available that validate the predictions of the model on the DC self bias and the rms values of the rf current which are decisive parameters for the ion energy and ion flux onto the substrate.[21,22] Clearly, more experimental research is required at various gas pressures, driving voltage amplitudes as well as driving frequencies.

In this paper, we want to critically re-examine the predictions of the nonlinear global model in the light of experimentally measured plasma parameters such as the electron density, temperature as well as the driving voltage amplitudes. To measure the plasma parameters in the 13.56 MHz CCP a rf compensated Langmuir probe is used. The rms values of discharge current and voltage at different experimental conditions are measured by using VI probes. The measured experimental parameters are then incorporated in the analytical model and the variation of the DC self bias and rf current as a function of the rf powers and pressures is studied. Moreover as the operational conditions include a wide range of pressures and rf powers, we hope that this study might be beneficial for a better understanding of the dynamics of the CCP discharge. The present investigation is organized as follows; the experimental set-up is introduced in Section II, predictions of the analytical treatment are outlined in Section III, results and discussions are mentioned in Section IV and the findings are summarized in Section V.

II. EXPERIMENTAL SET UP

The experiments were carried out in a geometrically asymmetric CCP driven by 13.56 MHz rf source, operating in argon gas. The experimental set up of the system is shown in Fig. 1. The electrode assembly of the rf discharge consists of two water cooled circular disc shaped parallel stainless steel electrodes separated by 7.5 cm. The diameter of the lower powered electrode is 8 cm and diameter of the upper grounded electrode is 10 cm.

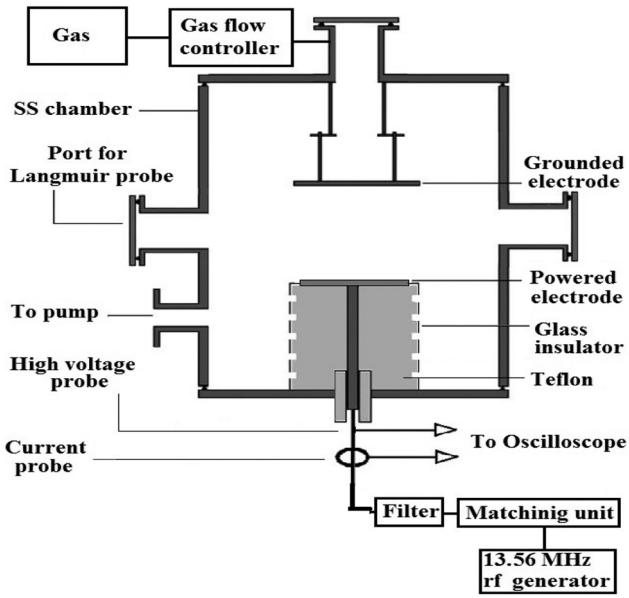

FIG. 1. Schematic diagram of the experimental set up.

The base pressure in the stainless steel vacuum chamber was maintained at 10^{-5} mbar with a combination of rotary and turbo molecular pumps. A mass flow controller is used to maintain the flow rates of argon into the chamber. The experiments were carried out at an argon pressure of 73-400 mTorr. The discharge current and voltage are measured by a Tektronix TCP0150 current probe and Tektronix HVP-15HF voltage probe. The current and voltage signals are recorded by a Tektronix DPO-4104 oscilloscope for further analysis. The voltage probe has very high impedance (100 MΩ/1 pF) and, therefore it is considered that the voltage probe hardly affects the voltage or current waveforms. The capacitance between the powered electrode and the grounded electrode is 0.55 pF (parasitic capacitance). The 13.56 MHz generator (ENI ACG-6B) can deliver up to a maximum of 600 W. Automatic L type matching network (ENI MWH-5-01) is connected in between the rf power supply and the electrodes to deliver maximum power to the plasma. The generator is equipped with a meter for simultaneously monitoring the forwarded and reflected power. To measure the electron density (n_e) and the electron temperature (T_e), a rf compensated Langmuir probe is used. The probe is placed in between the two electrodes through a movable feed through and can be positioned along a straight line centred between the electrodes. The probe tip is made of tungsten wire of 400 μm in diameter and 7 mm in length (exposed part in the plasma). To suppress the interference in the measured I-V curve brought about by the RF fluctuations of the plasma potential, passive rf filters are connected to the probe. Further compensation is achieved by the use of an external floating electrode (20 turns of 0.125 mm diameter tungsten wire wound around the probe insulator) which is connected to a point between the probe tip and the rf filters through a capacitor. The probe is biased with an amplified triangular wave of 120 V peak-to-peaks. A dc offset is added such that the probe voltage can be changed from –60 V to 120 V at a frequency of 10 Hz. The Langmuir probe measurements are carried out at a distance of 30 mm above the power electrode. The details of the rf compensation scheme is mentioned in our previous publications.[23] The amplitudes of the voltage waveform are determined at the powered electrode's surface via Fourier analysis and a calibration routine. This calibration procedure is performed by venting the chamber and attaching the high voltage probe to the powered electrode's surface. Comparisons of the voltage waveform amplitudes at the measurement point on the coaxial cable and at the electrode surface yield calibration factors for rf voltage amplitude. These calibration factors are strongly system dependent and are different for different applied frequencies. This calibration procedure is based on the assumption that the impedance of the plasma is similar to the impedance when the chamber is vented.[24] The high voltage probe and the oscilloscope are used to monitor the voltage waveform during plasma operation.

III. THE ANALYTICAL MODEL

In typical CCP discharges the length of the quasi-neutral bulk (l_p) is significantly larger than the time averaged sheath width ($\bar{s}$) so that the following ordering of length scales applies:

$$\lambda_D \langle\langle \bar{s} \langle\langle l_p \tag{1}$$

Here $\lambda_D = ((\varepsilon_0 k_B T_e)/(en_e))^{1/2}$ is the debye length.

Also, for CCP discharges operated in heavy gases at reasonable low plasma densities the following ordering of frequency scales applies:

$$\omega_{pi} \langle\langle \omega_{rf} \langle\langle \omega_{PSR} \langle \omega_{pe} \tag{2}$$

Here ω_{pi} is the ion plasma frequency, ω_{rf} is the applied radio frequency, ω_{PSR} is the plasma series resonance frequency and ω_{pe} is the electron plasma frequency. Under the conditions defined by Eqs. (1) and (2) a CCP discharge can be identified with an equivalent circuit in the frame of a global model. An electrical equivalent circuit of the nonlinear global model of the CCP discharge is shown in Fig. 2.[11–13] The external circuit consists of an ideal voltage source generator in series with a blocking capacitor, across which the DC self-bias is generated. The discharge itself consists of two non-linear capacitors representing the sheaths adjacent to both electrodes in series with an inductance (representing electron inertia) and a resistance (electron neutral collisions) representing the plasma bulk.

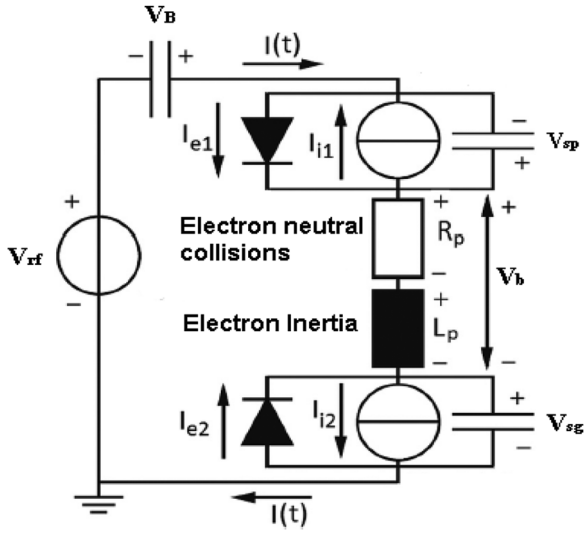

FIG. 2. Schematic diagram of the electrical circuit equivalent to the CCP discharges. Here I(t) represents the rf current, I_{e1} and I_{i1} represents the electron and ion current to the powered electrode sheath, and I_{e2} and I_{i2} represents the electron and ion current to the grounded electrode sheath.

The voltage balance equation of the CCP discharge in the frame of this model is,

$$V_{rf}(t) = V_{sp}(t) + V_{sg}(t) + V_B(t) + V_b(t) \tag{3}$$

where V_{rf} is the applied rf voltages, V_{sp} is the voltage drop across the powered electrode, V_{sg} is the voltage drop across the grounded electrode, V_B is the bias capacitor voltage and V_b is the voltage drop across the plasma bulk.

The plasma bulk is assumed to be quasineutral and for simplicity it is considered as homogeneous, $n_e = n_i = n$ = constant. Since $\omega_{rf} << \omega_{pe}$, the current in the plasma bulk is carried by electron conduction alone and the dependence of the current density on the electric field can, thus, be modeled by generalized Ohms law. It takes into account the acceleration of the electrons by the electric field and their momentum loss due to elastic collision with the neutrals of the background gas. The effective collision rate is given by,[14]

$$\nu_{eff} = \nu_m + \frac{\nu_e}{l_p} \tag{4}$$

where ν_m is the momentum transfer collision frequency and $\nu_e = \sqrt{\frac{8eT_e}{\pi m_e}}$ is mean thermal speed, where T_e is electron temperature in equivalent volt unit, m_e is the electron mass and l_p is the bulk plasma length. The factor is $\frac{\nu_e}{l_p}$ taken into account because of the fact that Stochastic heating plays a significant role in CCRF plasma along with Ohmic heating.

Various experimental and simulation studies in CCP discharge have shown that, the charge voltage characteristic for the sheath is quadratic to a good approximation and is given by,

$$|V_{s,m}| = \frac{Q_{s.m}^2}{2e\varepsilon_0 \bar{n}_{s,m} A_{s,m}^2} \tag{5}$$

with $Q_{s,m}$ and $A_{s,m}$ are the charge and area of the sheath (denoted by suffix s) and the suffix $m = p$ represents the sheath at the powered electrode while $m = g$ represents the sheath at the grounded electrode, respectively. $\bar{n}_{s,m}$ is the mean ion density in the sheath.[14–18] It is worthwhile to mention here that there are several reports available in literature where the deviation from the quadratic relation between the sheath charges and the voltages are considered.[21,22] In that case, the sheath charge and voltage relation were evaluated by solving the fluid equations. However, in our previous publication using this approach it was realized that the results do not have any significant difference, and so the Eq. (5) is used in present study.[18]

Assuming a Maxwell Boltzmann distribution for the electrons, the electron current from the bulk of the plasma to the sheath at the powered electrode and the grounded electrode are taken as $A_{s,p}j_e \exp(-\frac{Q_{s,p}^2}{2e\varepsilon_0\bar{n}_{s,p}A_{s,p}^2})$ and $A_{s,g}j_e \exp(-\frac{Q_{s,g}^2}{2e\varepsilon_0\bar{n}_{s,g}A_{s,g}^2})$ respectively, with $j_e = env_e$. The electron current is approximated by a reverse-biased diode as shown in Fig. 2. Similarly the ion current to the powered electrode and grounded electrode sheath are taken as $A_{s,p}j_i$ and $A_{s,g}j_i$ where $j_i = env_B$ with $v_B = \sqrt{\frac{k_BT_e}{M}}$ is the Bohm speed and M is the ion mass. In the radio-frequency range, the steady Bohm flux of ions in circuit terms has the appearance of a constant current source as shown in Fig. 2.

With all the approximations mentioned above, the circuit in Fig. 2 is now described by a set of four first order nonlinear differential equations for the sheath charge at the powered electrode ($Q_{s,p}$), the grounded electrode ($Q_{s,g}$), the bias capacitor voltage (V_B), and the radio frequency current ($I(t)$) as follows;[14–18]

$$\frac{dQ_{s,p}}{dt} = -(I(t) + A_{s,p}j_i - A_{s,p}j_e \exp(-\frac{Q_{s,p}^2}{2e\varepsilon_0\bar{n}_{s,p}A_{s,p}^2T_e})) \tag{6}$$

$$\frac{dQ_{s,g}}{dt} = -(-I(t) + A_{s,g}j_i - A_{s,g}j_e \exp(-\frac{Q_{s,g}^2}{2e\varepsilon_0\bar{n}_{s,p}A_{s,p}^2T_e} \times \frac{\bar{n}_{s,p}A_{s,p}^2}{\bar{n}_{s,g}A_{s,g}^2})) \tag{7}$$

$$\frac{dV_B}{dt} = -\frac{1}{C_B}(I(t)) \tag{8}$$

$$\frac{dI}{dt} = L^{-1}{}_p(\frac{1}{2e\varepsilon_0\bar{n}_{s,p}A_{s,p}^2}(Q^2{}_{s,p} - Q^2{}_{s,g} \times \frac{\bar{n}_{s,p}A_{s,p}^2}{\bar{n}_{s,g}A_{s,g}^2}) + V_{rf}(t) + V_B(t)) - v_{eff}I(t) \tag{9}$$

$L_p = \frac{l_pm_e}{e^2n_eA_{s,p}}$ represents the inductance of the plasma bulk. C_B is the value of the blocking capacitor across which the DC self bias is generated. The factor $\frac{\bar{n}_{s,p}A_{s,p}^2}{\bar{n}_{s,g}A_{s,g}^2}$ is known as the discharge symmetry parameter and is denoted by ε, i.e.

$$\varepsilon = \frac{\bar{n}_{s,p}A_{s,p}^2}{\bar{n}_{s,g}A_{s,g}^2} \tag{10}$$

As the Eqs. (6)–(9) are a set of ordinary differential equations; they are solved with MATLAB's ordinary differential equation solver. In the next section we are going to discuss the input parameters, namely the electron density, the electron temperature, the discharge symmetry parameter ε, and the applied rf voltage waveforms that are required to solve the above mentioned set of differential equations. The authors believe that the incorporation of these experimentally accessible parameters in to an non linear global model and attempt to predict the discharge dynamics considering both sheaths is a novel attempt in such discharges.

IV. RESULTS AND DISCUSSION

A. Input parameters of the model

In this section we determine the model input parameters that are capable of representing the real CCP experiment. The powered electrode has a radius of 4 cm and an area of $A_{s,p} = 50.24cm^2$. It is opposed by another electrode of radius 5 cm which acts as the closest grounded electrode. The electrode gap is 7.50 cm which is assumed to be equal to the bulk length of the plasma. In order to compare the measured value of the DC self bias with the output of the analytical model, one must incorporate the discharge symmetry parameter (ε) in the model.[25] The discharge symmetry parameter is related to the DC self bias voltage by the following equation;[25]

$$\langle V_B \rangle = -\frac{V_{m_1} + V_{m_2}}{1 + \varepsilon} \tag{11}$$

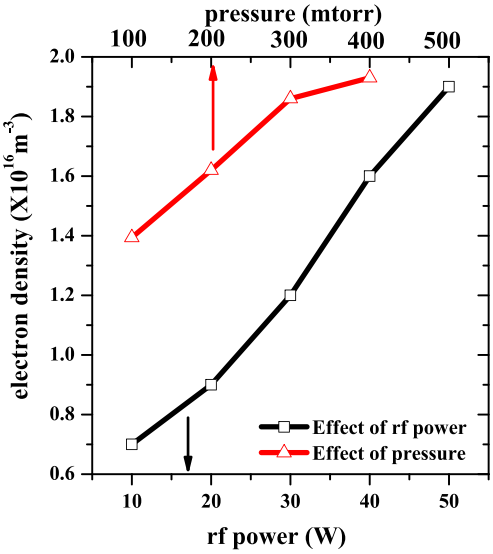

FIG. 3. Effect of rf power and working pressure on electron density.

In the present experimental conditions the measured values of ε are found to vary from 0.07 to 0.09. We have taken an average value of $\varepsilon = 0.08$ for the calculation of the outputs of the model. The value of the blocking capacitor is 3.34×10^{-9} F.

In order to determine the remaining input parameters in the 13.56 MHz CCP, two sets of experiments have been carried out. In one set the rf power was varied from 10W to 50W at an operating pressure of 73mTorr and, in an another set the operating pressure was varied from 100mTorr to 400mTorr, keeping the rf power constant at 50W. In the present experiment the electron temperature is derived from the linear part of the logarithmic electron current.[23] The effect of the rf power and the working pressure variations on the electron density is shown in the Fig. 3. It shows that the electron density increases from 0.7×10^{16} m $^{-3}$ to 1.9×10^{16} m $^{-3}$ as rf power increases from 10W to 50W, while it increases from 1.39×10^{16} m $^{-3}$ to 1.93×10^{16} m $^{-3}$ with the increase of working pressure from 100 to 400 mtorr.

The physical reason behind this increase in the density with the rf power is that in the α-mode, the rf source causes the sheath to expand more rapidly at high input power and it increases the electron density.[26] Next, we need to reconstruct the applied rf voltage waveform to the powered electrode. The voltage waveforms applied to the powered electrode is simulated in such a way that the peak to peak value of the applied voltage waveform (measured) and input voltage waveform (simulated) are same. It is given by,

$$V_{rf}(t) = V_0 \cos(2\pi \times 13.56 \times 10^6 t) \tag{12}$$

where V_0 is the amplitude of the applied voltage. Although in the present experimental set-up, it is not possible to determine the values of the mean ion density in the powered as well as the grounded electrode sheath, the ratio of mean ion density of the respective sheath is included in the measurement

TABLE I. Parameters for the solution of the differential equations at different rf powers.

n (in m^{-3})	T_e (in eV)	ν_{eff} (in s^{-1})	L_p^{-1} (kgm^2/c^2)$^{-1}$	$\frac{1}{2e\varepsilon_0 nA^2_{s,p}}$ (in V/C^2)	Power (in W)
0.7X10^{16}	1.1	2.493X10^8	1.32X10^7	1.97X10^{18}	10
0.9X10^{16}	1.1	2.493X10^8	1.69X10^7	1.53X10^{18}	20
1.2X10^{16}	1.2	2.497X10^8	2.26X10^7	1.15X10^{18}	30
1.6X10^{16}	1.1	2.493X10^8	3.0X10^7	8.62X10^{17}	40
1.90X10^{16}	1.0	2.40X10^8	3.58X10^7	7.26X10^{17}	50

TABLE II. Parameters for the solution of the differential equations at different working pressures at rf power of 50W.

n (in m^{-3})	T_e (in eV)	L_p^{-1} $(kgm^2/c^2)^{-1}$	$\frac{1}{2e\varepsilon_0 nA^2_{s,p}}$ (in V/C^2)	ν_{eff}
$1.39X10^{16}$	1.37	$2.63X10^7$	$9.89X10^{17}$	$3.3X10^8$
$1.62X10^{16}$	1.34	$3.05X10^7$	$8.51X10^{17}$	$6.6X10^8$
$1.86X10^{16}$	1.33	$3.60X10^7$	$7.41X10^{17}$	$9.9X10^8$
$1.93X10^{16}$	1.39	$3.64X10^7$	$7.15X10^{17}$	$13.20X10^8$

of ε. In the frame of the global model, it is assumed that the value of the mean ion density in the powered electrode sheath is equal to the bulk electron density. The remaining parameters that are required to solve the Eqs. (6)–(9) are mentioned in the Tables I and II, respectively.

B. Model results

Now that all the input parameters required for solving the equations are mentioned in the Tables I and II, we can determine the outputs the analytical model, namely $V_B(t)$, $I(t)$ and $Q_{s,p}(t)$. The variation of V_B as a function of the rf powers and pressures is shown in Fig. 4. The time average value of V_B yields the DC self bias voltage. It represents the difference between the time averaged sheath potential at the powered electrode and the grounded electrode. It is compared with the experimentally measured DC self bias voltage at different experimental conditions and is shown Fig. 5. Very good agreement between the measured values of the DC self bias voltage with the ones determined from the model were found with a deviation less than 7.57%. In view of the certain limitations of the model such as the assumption of a constant inertial term, equivalence of the bulk electron and mean ion density in the powered electrode sheath, this is a very good agreement. However, with the increase of the pressure, the maximum discrepancy between them increases to about 9% at 100mtorr.

To study the dynamics of the CCP, we have plotted the charge in the sheath at the powered electrode ($Q_{s,p}$) and rf current (I) as a function of time in Fig. 6. In a typical CCP discharge when the applied rf voltage is minimum the powered electrode sheath is extended and the sheath charge is high; when the rf voltage is maximum, the sheath collapses resulting in a small sheath charge. The rapid expansion observed (shown by the arrow in the Fig. 6) during the moment of the sheath collapse is a clear indication of the excitation of the plasma series resonance effect.[11,14] A more detailed analysis of the PSR effect is done via Fourier Transform of the current waveform obtained from the numerical model and is shown in the Fig. 7. It reveals that PSR oscillations lead to a broad frequency spectrum. The Fourier component at the applied frequency of 13.56 MHz is clearly visible. D. Ziegler *et al.* have classified such a non linear global plasma model as a 'driven nonlinear oscillator with dissipation'

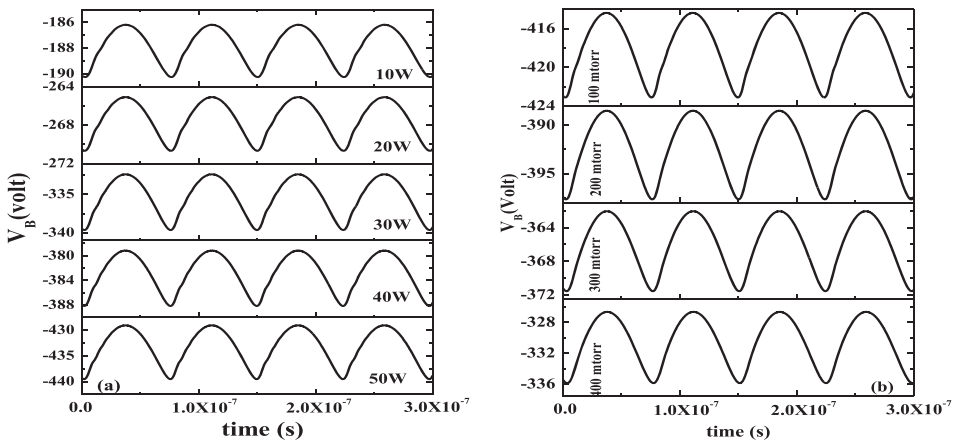

FIG. 4. The variation of the $V_B(t)$ as a function of the rf power (a), and the working pressure (b).

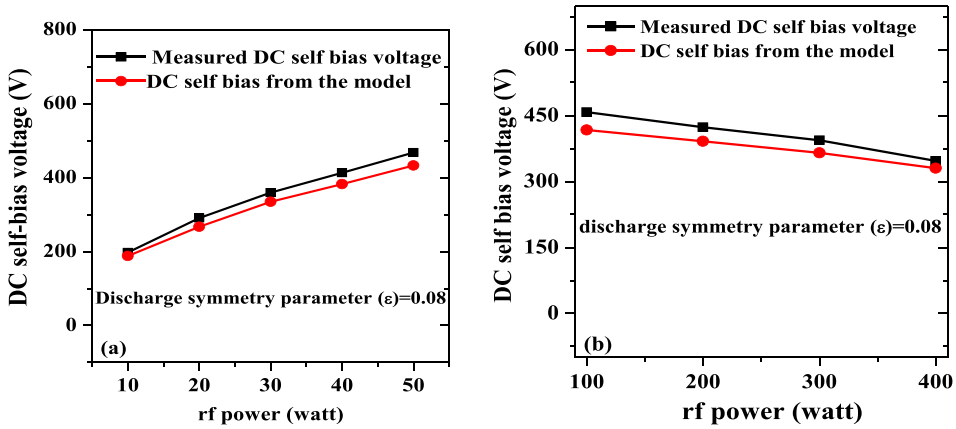

FIG. 5. The comparison of the experimentally measured and calculated values of the DC self bias voltage as a function of the rf power (a), and the pressure (b).

with resonance frequency of this oscillator is that of the plasma series resonance ω_{PSR}.[22] The sharp resonance observed (Fig. 7) around the 11st harmonics of the 13.56 MHz frequency may corresponds to the PSR frequency at 73 mtorr. At high pressures, no PSR oscillations are excited efficiently due to the strong collision damping.

In order to observe this nonlinear effect experimentally, the rf current density to the grounded chamber wall can be measured by a SEERS (Self Excited Electron Plasma Resonance Spectroscopy) current sensor.[13] This is outside the scope of the present investigation. This prevents us from

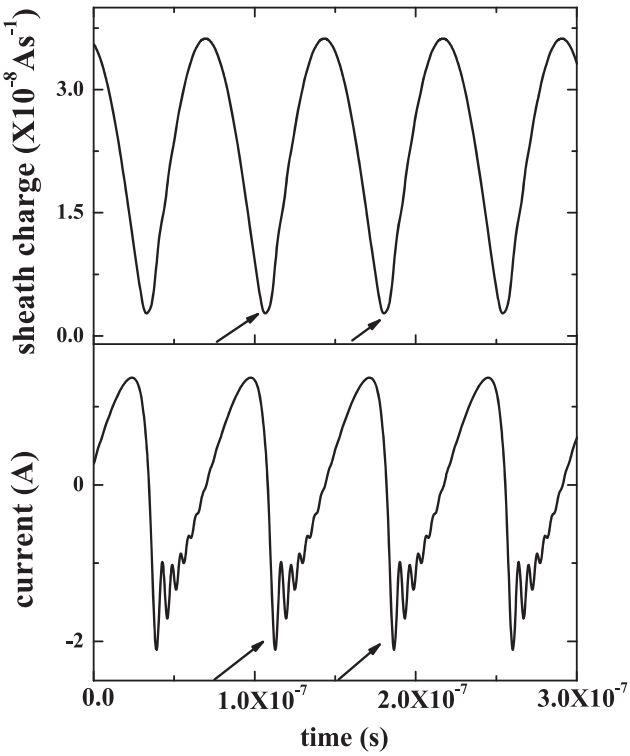

FIG. 6. The variation of the charge in the sheath at the powered electrode ($Q_{s,p}(t)$) and rf current (I) obtained from the non linear model with time at P =50W and pressure 73 mtorr. The excitation of the PSR is observed at the moment of sheath collapse (shown by the arrow).

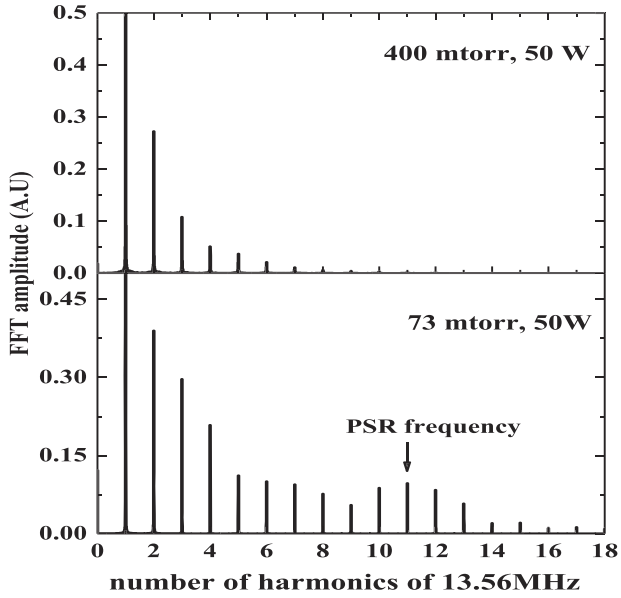

FIG. 7. Fast fourier transforms (FFTs) of the rf current waveforms obtained from the analytical model at different working pressure.

comparing the experimental results to those of the numerical model. But, we can compare the rms values of the radio frequency current (I) measured by the VI probe with the values calculated by the numerical model. At low working pressures the simulated and the experimentally measured values of the rms current shows good agreement (Fig. 8). However with the increase in the pressure, the experimentally measured values deviate from the simulated values. This may be due to effect of the secondary electrons that are accelerated and multiplied most effectively inside the power electrode sheath by collisions at high pressure.[26,27] Since these electrons are not taken into account in the present numerical modeling, therefore the observed discrepancy between the numerical model and the experimental data is observed at the higher pressure.

We conclude that the model output parameters agree well with the experimentally measured values. The authors acknowledge the fact that the non-linear global model is analytically non self-consistent compared to the self consistent PIC/MCC. However, it has various advantages as already mentioned in the manuscript. In particular, with the experimentally measured values of the

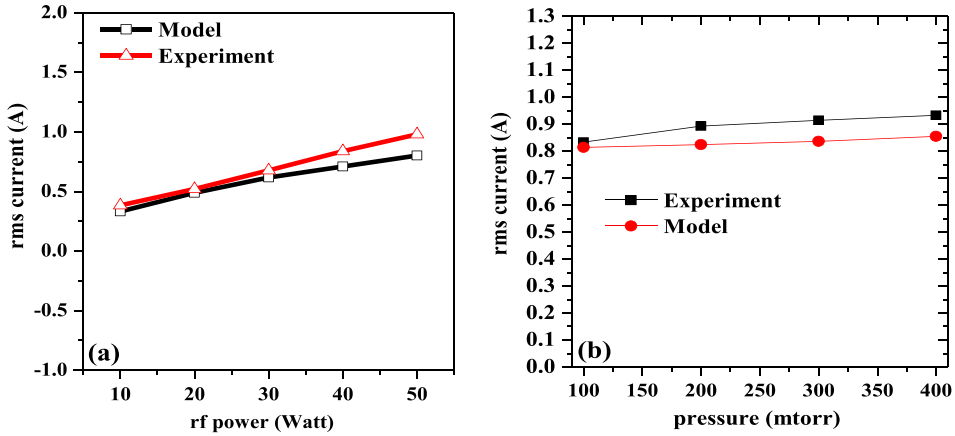

FIG. 8. The comparison of the experimentally measured and rms values of the rf current (I) computed from the model as a function of the radio frequency power at 73 mtorr (a), and the working pressure (b).

electron density, the electron temperature and discharge symmetry parameter; this model could be used most promptly to determine the DC self bias, the voltage drop across the powered as well as the grounded electrode, and also the discharge current in the reactor. These information are very useful for a multitude of processing techniques such as plasma etching, pulsed laser deposition in the background of rf plasmas, and rf magnetron sputtering. Although we have applied the analytical model to the single frequency CCP in principle, it could be applied to dual or multi-frequency CCP at different operating conditions. We are presently working on the experimental validation of the dual frequency geometrically asymmetric discharge using this analytical model and will be reported in due course.

V. CONCLUSION

In this manuscript, we experimentally studied the behavior of geometrically asymmetric capacitively coupled plasma driven by 13.56 MHz rf sources. We started by increasing the radio frequency power by keeping the operating pressure constant at 73mtorr constant and then, the operating pressure was varied from 100m Torr to 400mTorr keeping the rf power constant at 50W. The variation of the electron temperature as well as the electron density was found using a rf compensated Langmuir probe. The voltage amplitude was derived from the FFT of the voltage waveform. The value of the DC self bias and rms value of the rf current was measured at different operating conditions. We then used the measured values of the electron density, the electron temperature, the discharge symmetry parameters and voltage amplitudes as the input parameters of a non linear global model of the CCP discharge to obtain the value of the DC self bias and the rf current as the output parameters. A good quantitative correspondence between the measured value of the DC self bias with the ones determined from the model was found. A closer investigation of the modeled rf current waveforms reveals that the self excitation of the plasma series resonance oscillation which is triggered at the moment of the sheath collapse. Although the detection of such PSR oscillations experimentally is beyond the scope of the present work, the measured and calculated rms values of the rf current show a similar modulation as function of the rf power and operating pressures.

ACKNOWLEDGMENTS

Authors acknowledge FONDECYT grant 1170261 and 3160179. Many helpful suggestions from Dr. J. Schulze while preparing the manuscript are also acknowledged.

[1] A. Grill, *Cold Plasma Material Fabrication: From Fundamentals to Applications* (IEEE, NJ, 1993).
[2] N. Spiliopoulos, D. Mataras, and D. E. Rapakoulias, J. Vac. Sci. Technol. A **14**(5), 2757 (1996).
[3] M. A. Liberman and A. J. Lichtenberg, *Principles of Plasma Discharges and Materials Processing*, 2nd ed. (Wiley, NJ, 2005).
[4] H. Curtins, N. Wyrsch, M. Favre, and A. V. Shah, Plasma Chem. Plasma Process. **7**, 267 (1987).
[5] K. Ostrikov, Rev. Modern Physics **77**, 489 (2005).
[6] K. H. Becker, U. Kogelschatz, K. H. Schoenbach, and R. J. Barker, *Non-Equilibrium Air Plasmas at Atmospheric Pressure* (Institute of Physics Publishing, Bristol, 2005).
[7] E. Valderrama, M. Favre, H. Bhuyan, H. M. Ruiz, E. Wyndham, J. Valenzuela, and H. Chuaqui, Surf. Coat. Technol. **204**, 2940 (2010).
[8] M. L. Hoey, J. B. Carlson, R. M. Osgood, B. Kimball, and W. Buchwald, Appl. Phys. Lett. **97**, 153104 (2010).
[9] M. Wojtaszek, N. Tombros, A. Caretta, P. H. Loosdrecht, and H. J. Wess, J. Appl. Phys. **110**, 063715 (2011).
[10] A. Mishra, M. H. Jeon, K. N. Kim, and G. Y. Yeom, Plasma Sources Sci. Technol. **21**, 055006 (2012).
[11] U. Czarnetzki, T. Mussenbrock, and R. P. Brinkmann, Phys. Plasmas. **13**, 123503 (2006).
[12] T. Mussenbrock and R. P. Brinkmann, Appl. Phys. Lett. **88**, 151503 (2006).
[13] M. J. Klick, J. Appl. Phys. **79**, 3445 (1996).
[14] T. Mussenbrock, R. P. Brinkmann, M. A. Libermann, A. J. Lichtenberg, and E. Kawamura, Phys. Rev. Lett. **101**, 085004 (2008).
[15] B. Bora, H. Bhuyan, M. Favre, E. Wyndham, and H. Chuaqui, Appl. Phys. Lett. **100**, 094103 (2012).
[16] B. Bora, H. Bhuyan, M. Favre, E. Wyndham, and C. S. Wong, J. Appl. Phys. **113**, 153301 (2013).
[17] B. Bora and L. Soto, Phys. Plasmas **21**, 083509 (2014).
[18] B. Bora, Phys. Plasmas. **22**, 103503 (2015).
[19] A. Derzsi, E. Schungel, Z. Donkó, and J. Schulze, Open Chemistry **13**, 346 (2015).
[20] Z. Donkó, J. Schulze, U. Czarnetzki, A. Derzsi, P. Hartmann, I. Korolov, and E. Schüngel, Plasma Phys. Contr. Fusion **54**, 124003 (2012).
[21] E. Semmler, P. Awakowicz, and A. V. Keudell, Plasma Sources Sci. Technol. **16**, 839 (2007).

[22] D. Ziegler, T. Mussenbrock, and R. P. Brinkmann, Plasma Sources Sci. Technol. **17**, 045011 (2008).
[23] P. Saikia, H. Bhuyan, M. Favre, E. Wyndham, and F. Veloso, Phys. Plasmas **24**, 013503 (2017).
[24] J. Schulze, E. Schüngel, and U. Czarnetzski, J. Phys. D: Appl. Phys **42**, 092005 (2009).
[25] B. G. Heil, U. Czarnetzki, R. P. Brinkmann, and T. Mussenbrock, J. Phys. D: Appl. Phys. **41**, 165202 (2008).
[26] J. Schulze, E. Schungel, U. Czarnetzki, M. Gebhardt, R. P. Brinkmann, and T. Mussenbrock, Appl. Phys. Lett. **98**, 031501 (2011).
[27] A. Derzsi, I. Korolov, E. Schungel, Z. Donkó, and J. Schulze, Plasma Sources Sci. Technol. **22**, 065009 (2013).